Spectroscopic and Quantum Chemical Studies of Excited States of One- and Two-Electron Oxidation Products of a Lutetium Triple-Decker Phthalocyanine Complex

Naoto Ishikawa,* Tomoko Okubo, and Youkoh Kaizu

Department of Chemistry, Tokyo Institute of Technology, O-okayama, Meguro-ku, Tokyo, 152-8551, Japan

Received December 22, 1998

Electronic and MCD (magnetic circular dichroism) spectra of dilutetium(III) tris(phthalocyanate), $Lu_2(Pc)_3$ (Pc = phthalocyanine), its one-electron oxidation product $[Lu_2(Pc)_3]^+$, and its two-electron oxidation product $[Lu_2(Pc)_3]^{2+}$ are reported. $Lu_2(Pc)_3$ was prepared by a new synthetic route in which $PcLu(CH_3COO)(H_2O)_2$ is used as the starting material. This new route enabled a purification of the triple-decker compound to a level necessary for spectroscopic measurements. Each of the two chemical oxidation steps occurred keeping isosbestic points. The first oxidation product $[Lu_2(Pc)_3]^+$ shows a relatively intense band in the near-IR region. This is assigned to the LUMO-to-SOMO (singly occupied orbital) transition. The band has a transition moment perpendicular to the Pc planes. A single intense band was observed in the Q-band region in $[Lu_2(Pc)_3]^+$ in contrast to the two bands in $Lu_2(Pc)_3$. Between the Q band and the near-IR band, several weak bands are observed. Among them, two bands show clear MCD *A*-term dispersions. In the region between the Q band and the B band, $[Lu_2(Pc)_3]^+$ shows a characteristic band for Pc π radicals. Its MCD pattern suggests the presence of a negative *A* term. The second oxidation product $[Lu_2(Pc)_3]^{2+}$ displays an intense band with two distinct vibronic bands in the near-IR region. None of the bands in the region shows an *A*-term contribution in MCD. The Q band remains single. There is only one band which shows an MCD *A* term between the near-IR band and the Q band. Semiempirical quantum chemical calculations were carried out for the ground and excited states of $[Lu_2(Pc)_3]^+$ and $[Lu_2(Pc)_3]^{2+}$. Band assignments are discussed using the theoretical excitation energies, oscillator strengths, and MCD *A* terms.

Introduction

Triple-decker complexes composed of phthalocyanines (Pc) and/or porphyrins have been reported by many researchers.[1−5] Oxidation of a complex of this type results in a hole with a population pattern depending on the combination of the macrocycles.[5b] One of the important electronic-spectral features of the oxidized macrocycle stacks is the intense absorption band[4d,5c,d,6,8] which appears in the NIR (near-IR) region. An excitation of the band has a transition moment perpendicular to the planes on which macrocycles lie and induces a displacement of the hole population among the macrocycles. The movement of the hole can be viewed as a model of the electric conduction in doped Pc crystals whose valence bands are partially filled.[11] In the triple-decker complexes, a succeeding oxidation results in a system having two holes per three macrocycles. Such a system corresponds to a Pc crystal with increased dopant.

In discussing the nature of the electronic excitations in the multilayered systems, the complexes containing only Pc macrocycles have one advantage over those containing porphyrins. The lowest excited state of a Pc monomer is described predominantly by HOMO-to-LUMO excited configuration because the HOMO and LUMO are relatively isolated in energy from the rest of the orbitals.[12,13] The excited states of Pc multilayered complexes below the Q-band region are effectively described on the basis of the MOs composed of the HOMO and LUMO of the monomer. On the other hand, porphyrins have accidentally degenerate HOMOs, which necessitate at least four orbitals to describe the lowest excited states of the

(1) Kirin, I. S.; Moskalev, P. N.; Ivannikova, N. V. *Russ. J. Inorg. Chem.* **1967**, *12*, 497.
(2) M'Sadak, M.; Roncali, J.; Garnier, F. *J. Chim. Phys.* **1986**, *83*, 211.
(3) Kasuga, K.; Ando, M.; Morimoto, H.; Isa, M. *Chem. Lett.* **1986**, 1095.
(4) (a) Buchler, J. W.; De Cian A.; Fischer, J.; Kihn-Botulinski, M; Paulus, H.; Weiss, R. *J. Am. Chem. Soc.* **1986**, *108*, 3652. (b) Buchler, J. W.; De Cian A.; Fischer, J.; Kihn-Botulinski, M; Weiss, R. *Inorg. Chem.* **1988**, *27*, 339. (c) Buchler, J. W.; Kihn-Botulinski, M; Löffler, J.; Wicholas, M. *Inorg. Chem.* **1989**, *28*, 3770. (d) Duchowski, J. K.; Bocian, D. F. *J. Am. Chem. Soc.* **1990**, *112*, 8807. (e) Buchler, J. W.; Kihn-Botulinski, M.; Löffler, J.; Scharbert, B. *New J. Chem.* **1992**, *16*, 545.
(5) (a) Chabach, D.; Lachkar, M.; De Cian, A.; Fischer, J.; Weiss, R. *New J. Chem.* **1992**, *16*, 431. (b) Tran-Thi, T.-H.; Mattioli, T. A.; Chabach, D.; De Cian, A.; Weiss, R. *J. Phys. Chem.* **1994**, *98*, 8279. (c) Chabach, D.; Tahiri, M.; De Cian, A.; Fischer, J.; Weiss, R.; El Malouli Bibout, M. *J. Am. Chem. Soc.* **1995**, *117*, 8548. (d) Chabach, D.; De Cian, A.; Fischer, J.; Weiss, R.; El Malouli Bibout, M. *Angew. Chem., Int. Ed. Engl.* **1996**, *8*, 35. (e) Jiang, J.; Lau, R. L. C.; Chan, D.; Mak, T. C. W.; Ng, D. K. P. *Inorg. Chim. Acta* **1997**, *255*, 59.
(6) Takahashi, K.; Itoh, M.; Tomita, Y.; Nojima, K.; Kasuga, K.; Isa, K. *Chem. Lett.* **1993**, 1915.
(7) Ishikawa, N.; Kaizu, Y. *Chem. Phys. Lett.* **1994**, *228*, 625.
(8) Ishikawa, N.; Kaizu, Y. *Chem. Phys. Lett.* **1994**, *236*, 50.
(9) Takahashi, K.; Shimoda, J.; Itoh, M.; Fuchita, Y.; Okawa, H. *Chem. Lett.* **1998**, 173.
(10) Ishikawa, N.; Kaizu, Y. *J. Phys. Chem.* **1996**, *100*, 8722.
(11) (a) Yakushi, K.; Yamakado, H.; Yoshitake, M.; Kosugi, N.; Kuroda, H.; Kawamoto, A.; Tanaka, J.; Sugano, T.; Kinoshita, M.; Hino, S. *Synth. Met.* **1989**, *29*, F95. (b) Hino, S.; Matsumoto, K.; Yamakado, H.; Yakushi, K.; Kuroda, H. *Synth. Met.* **1989**, *32*, 301.
(12) (a) Weiss, C.; Kobayashi, H.; Gouterman, M. *J. Mol. Spectrosc.* **1965**, *16*, 415. (b) McHugh, A. J.; Gouterman, M.; Weiss, C., Jr. *Theor. Chim. Acta* **1972**, *24*, 346. (c) Henriksson, A.; Roos, B.; Sundbom, M. *Theor. Chim. Acta* **1972**, *27*, 303.
(13) Ishikawa, N.; Maurice, D.; Head-Gordon, M. *Chem. Phys. Lett.* **1996**, *260*, 178.

10.1021/ic981463x CCC: $18.00
Published on Web 06/08/1999

monomer.[14] Therefore multilayered complexes involving porphyrins require more orbitals to describe their lowest excited states below the Q-band region. Additionally, the strong vibronic coupling in the Q band of porphyrins makes the spectra of the multilayered complexes more complicated.[14] Studies on the absorption bands of the Pc triple-decker complexes should serve as fundamentals for understanding of the porphyrin−Pc mixed[5] and porphyrin-only[4] systems.

In spite of the importance of the Pc triple-decker complexes, only few reports on spectral measurements of the compounds have been published. This is in part because of their low solubility in organic solvents and the resultant difficulty in purification. Some attempts to increase solubility by introducing bulky substituents to Pc have been reported. Takahashi et al. reported the synthesis of triple-decker complexes of octabutoxyphthalocyanine.[6,9] We synthesized a heteroleptic complex (Pc)Lu(CRPc)Lu(Pc) (CRPc = 4,5:4′,5′:4″,5″:4‴,5‴-tetrakis-(1,4,7,10,13-pentaoxatridecamethylene)phthalocyanine) and showed the presence of weak electronic bands in the NIR region.[7] Electronic structure as well as assignment of the absorption bands of the neutral triple-decker complex has been studied by means of semiempirical quantum chemical calculations.[10]

The peripheral substitution does not significantly change the energies and profiles of the bands in the NIR and Q-band region. However, the alkoxyl groups directly attached to the Pc ring give rise to intense bands in the region from 400 nm up to the B band. The bands overlap the B band of Pc complexes and make it difficult to identify Pc-centered bands. The situation becomes worse when dealing with oxidized species: the "fingerprint band", which indicates an occurrence of an oxidation on Pc ligand,[8] is also partially covered by the extra bands. Due to the overlap, identification of Pc-centered bands of $[(Pc)Lu(CRPc)Lu(Pc)]^+$ above 20×10^3 cm^{-1} has not been completed.

The synthesis of an unsubstituted Pc triple-decker complex was first reported by Kirin for $Nd_2(Pc)_3$.[1] The triple-decker structure was first proposed by M'Sadak et al.[2] Kasuga et al. have reported that $Y_2(Pc)_3$ gives two distinct absorption bands in the Q-band region.[3] All of these reports employed a one-pot reaction whose starting materials were lanthanide acetate and dicyanobenzene. Although simple to apply, the method has a drawback: it inevitably produces fair amounts of byproducts such as monomer, dimer, and metal-free compounds, and it produces a very hard solid which is difficult to treat. In fact none of the reported spectra seems free from the byproducts.

In this paper, we present a new synthetic route to an unsubstituted Pc trimer $Lu_2(Pc)_3$ (Figure 1). This method enables an easier purification by chromatographic means. Then we present the results of detailed absorption and MCD (magnetic circular dichroism) spectrum measurements of $Lu_2(Pc)_3$, its one-electron-oxidized form $[Lu_2(Pc)_3]^+$, and its two-electron-oxidized form $[Lu_2(Pc)_3]^{2+}$. The measurements were carried out over the UV−vis−NIR region. Using semiempirical SCF-MO-CI calculations, electronic structures of the ground and excited states of the oxidized species are discussed.

Experimental Section

Synthesis of $Lu_2(Pc)_3$. Lutetium phthalocyanine acetate $PcLu(CH_3COO)(H_2O)_2$ (0.5 g), which was obtained by a method in the literature,[15] was heated at 400 °C for 4 h in vacuo (ca. 1 Torr) in a conventional sublimation tube equipped with a water-cooled inner trap. The solid remaining in the tube was extracted with dichloromethane. The solution was identified as a mixture of $Lu_2(Pc)_3$ and a small amount of $Lu(Pc)_2$ by UV−vis spectrum measurement. The solution was treated with hydrazine monohydrate to reduce $Lu(Pc)_2$ to $[Lu(Pc)_2]^-$ and was passed through a silica gel column (Merck silica gel 60, ca. 5 cm length) to remove the anionic $[Lu(Pc)_2]^-$. A hydrazine monohydrate layer was kept on top of the solution in the column to avoid oxidation of $[Lu(Pc)_2]^-$. The solution was washed with water, dried by magnesium sulfate, concentrated by evaporation, and added to hexane to give a microcrystalline powder of $Lu_2(Pc)_3$. The absence of possible byproducts such as $Lu(Pc)_2$, $[Lu(Pc)_2]^-$, PcH_2, and $PcLu(CH_3COO)(H_2O)_2$ was confirmed by a second-derivative absorption spectrum. Yield: 0.20 g (40%). Anal. Calcd for $C_{96}N_{24}H_{48}Lu_2$: C, 61.09; H, 2.56; N, 17.81; Lu, 18.54. Found: C, 60.78; H, 2.52; N, 17.77.

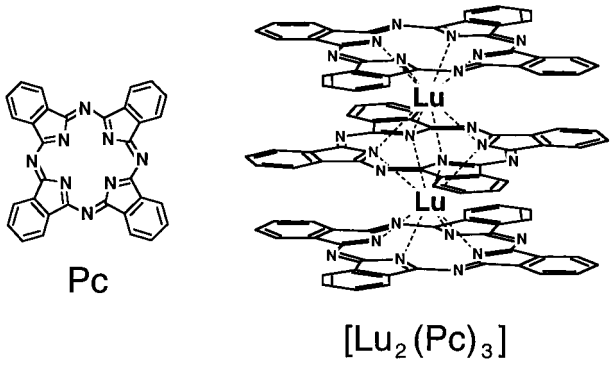

Figure 1. Schematic molecular structure of $Lu_2(Pc)_3$.

Oxidation of $Lu_2(Pc)_3$. $[Lu_2(Pc)_3]^+$ was obtained by an oxidation of $Lu_2(Pc)_3$ by addition of equimolar amounts of phenoxathiin hexachloroantimonate. A typical procedure was as follows: to 2 ml of $Lu_2(Pc)_3$ solution (5.1×10^{-6} M in dichloromethane) in a quartz cell with a 1 cm path length was added the oxidant (5.1×10^{-5} or 1.0×10^{-6} M in dichloromethane) fractionally by a microsyringe. The concentration of the oxidant was controlled and confirmed by the absorbance at 590 nm just before use. Two-electron-oxidation product $[Lu_2(Pc)_3]^{2+}$ was obtained by a subsequent addition of the oxidant.

Dichloromethane used for the oxidation and spectroscopic measurements was distilled, dried with calcium chloride, and fractionally distilled over calcium hydride. Phenoxathiin hexachloroantimonate was synthesized by a method described in the literature.[16]

Spectroscopic Measurements. UV−vis−NIR absorption spectra were measured on a Shimadzu UV-3100PC spectrophotometer. MCD spectra in the UV−vis region were taken on a JASCO spectropolarimeter J-500C in an external magnetic field set at 1 T, and those in the NIR region were taken on a JASCO J-730 with the magnetic field set at 1.5 T. ESR spectra were recorded on a JEOL JES-RE1X spectrometer operating at X-band frequency.

Theoretical Calculations

***π*-Electron Systems of the Trimer.** MO calculations of the Pc trimer were carried out within the π approximation using a semiempirical method.[18−20] The ground states of the closed-shell species $Lu_2(Pc)_3$ and $[Lu_2(Pc)_3]^{2+}$ were treated by the restricted Hartree−Fock (RHF) method.[17] The open-shell $[Lu_2(Pc)_3]^+$ was dealt with by the restricted open-shell Hartree−Fock (ROHF) method,[17] in which a single set of spatial functions

(14) Gouterman, M. In *The Porphyrins*; Dolphin, D., Ed.; Academic Press, Inc.: New York, 1978; Vol. III, pp 1−165.
(15) De Cian A.; Moussavi, M.; Fischer, J.; Weiss, R. *Inorg. Chem.* **1985**, *24*, 3162.
(16) Gans, P.; Marchon, J.-C.; Reed, C. A.; Regnard, J.-R. *Nouv. J. Chim.* **1981**, *5*, 203.
(17) McWeeny, R. *Method of Molecular Quantum Mechanics*, 2nd ed.; Academic Press Inc.: London, 1992; Chapter 6.
(18) Ohno, O.; Ishikawa, N.; Matsuzawa, H.; Kaizu, Y.; Kobayashi, H. *J. Chem. Phys.* **1989**, *93*, 1713.
(19) Ishikawa, N.; Ohno, O.; Kaizu, Y.; Kobayashi, H. *J. Phys. Chem.* **1992**, *96*, 8832.
(20) Ishikawa, N.; Ohno O.; Kaizu, Y. *J. Phys. Chem.* **1993**, *97*, 1004.

is used for both α and β spin−orbitals. Parameters[21−23] and formulas to evaluate molecular integrals used for the calculation were the same as those used previously for Pc monomer,[18] dimer,[19,20] and neutral trimer.[10] Two-electron interactions between two centers within a macrocycle at a distance r were evaluated with the formula prescribed by Nishimoto and Mataga[25] ($e^2/(a + r)$) which reasonably reproduced monomer Q and B bands. For the one-center Coulomb interaction e^2/a, we used the values determined by Gouterman et al.[12a,b,21] The interactions between two centers on different macrocycles were scaled as $\alpha e^2/(a + r)$, in which α is a parameter.[10,19,20] In this paper, α = 0.8, which best reproduced the Q bands of $[Lu(Pc)_2]^-$, was employed.[19] The geometry of $Lu_2(Pc)_3$ was approximated as a set of three Pc macrocycles being placed in parallel with a common C_4 axis. The interplanar distance was varied from 2.9 to 3.3 Å. The orientational angle between adjoining Pc rings around the axis was assumed to be similar to that of $Lu(Pc)_2$[15] or $[Lu(Pc)_2]^-$ [25] and set at 45°, giving a D_{4h} structure. The Lu ions were treated as +3 point charges. The charges were assumed to be neutralized by charge donation from the coordinated nitrogen atoms[23] so that the total metal charge was equally distributed among three Pc rings.

Excited States. Singlet excited states of the closed-shell species $[Lu_2(Pc)_3]^{2+}$ were calculated by the CIS method (configuration interaction of single excitations). The calculations took into account 189 excited configurations generated by promoting an electron from one of the 27 highest doubly occupied orbitals to one of the seven lowest virtual orbitals.

Doublet excited states of the open-shell $[Lu_2(Pc)_3]^+$ were calculated by a method equivalent to what is referred to as "XCIS" [26] (extended restricted open-shell CIS). The ROHF ground state ($|G\rangle$), from which excited configurations are constructed, is

$$|G\rangle = |...i\bar{i}...m|$$

and the singly excited configurations included in the calculations are

$$|D\ m \leftarrow i\rangle = |...i\bar{m}...m| \quad (1)$$

$$|D\ a \leftarrow m\rangle = |...i\bar{i}...a| \quad (2)$$

$$|S\ a \leftarrow i\rangle = \{|...a\bar{i}...m| - |...\bar{a}i...m|\}/\sqrt{2} \quad (3)$$

$$|T\ a \leftarrow i\rangle = \{2|...ai...\bar{m}| - |...a\bar{i}...m| - |...\bar{a}i...m|\}/\sqrt{6} \quad (4)$$

Here m, i, and a denote the singly occupied orbital (SOMO), an occupied orbital, and a virtual orbital, respectively. The method generates correct eigenfunctions of the total spin operator. The calculations in the present paper used 344 excited configurations involving six lowest virtual orbitals, one SOMO, and 26 highest doubly occupied orbitals.

MCD *A*/*D* Ratios. The MCD A term and the square of the transition moment D of a doubly degenerate excited state of E representation are calculated by the following equations:

$$A_a = -\frac{1}{2}\{\langle a|\hat{l}_z|a\rangle - \langle G|\hat{l}_z|G\rangle\}\ \mathrm{Im}\{\langle G|\hat{m}_x|a\rangle\langle a|\hat{m}_y|G\rangle - \langle G|\hat{m}_y|a\rangle\langle a|\hat{m}_x|G\rangle\}$$

$$D_a = \langle G|\hat{m}_x|a\rangle\langle a|\hat{m}_x|G\rangle + \langle G|\hat{m}_y|a\rangle\langle a|\hat{m}_y|G\rangle$$

Here $\hat{m}_x$ and $\hat{m}_y$ are electric dipole operators and $\hat{l}_z$ is an orbital angular momentum operator. The z axis was set along the C_4 axis of the molecule. The contributions of spin angular moments are not included in the equation for the A term since in this paper only excited states having the same spin quantum numbers as the ground state are discussed. The index a refers to the excited state in a complex form,

$$|a\rangle = (|a_x\rangle + i|a_y\rangle)/\sqrt{2}$$

or

$$|a\rangle = (|a_x\rangle - i|a_y\rangle)/\sqrt{2}$$

$|a_x\rangle$ and $|a_y\rangle$ are the two components of the degenerate excited state in real forms. Matrix elements in the AO basis for the angular momentum operator

$$\hat{l}_z = -i\hbar\left(x\frac{\partial}{\partial y} - y\frac{\partial}{\partial x}\right)$$

are calculated with the origin fixed at the center of the complex.

Results and Discussion

$Lu_2(Pc)_3$. Figure 2 shows absorption and MCD spectra of $Lu_2(Pc)_3$ in dichloromethane solution. In the Q-band region, two bands are observed at 15.9×10^3 cm^{-1} (628 nm) and 13.9×10^3 cm^{-1} (717 nm). A vibronic structure of the former band is seen at 17.5×10^3 cm^{-1}. The profiles of the bands in this energy region are quite similar to those of (Pc)Lu(CRPc)Lu(Pc).[7] Both the 15.9×10^3 and 13.9×10^3 cm^{-1} bands show MCD A-term dispersions. This indicates that each band corresponds to a transition to a degenerate excited state.

The "tail" extending from 13×10^3 to 10×10^3 cm^{-1} corresponds to the weak bands observed in (Pc)Lu(CRPc)Lu(Pc) at 11.6×10^3 and 10.2×10^3 cm^{-1}.[7] A band similar to the weak band of (Pc)Lu(CRPc)Lu(Pc) at 7×10^3 cm^{-1} was expected to be observed, but in the present case the low solubility and the interference from the solvent prevented detection of such a band.

In the B-band region, a single band with a maximum at 29.8×10^3 cm^{-1} (336 nm) is observed. The band showed a clear MCD A term. This is quite different from the corresponding B-band manifold of (Pc)Lu(CRPc)Lu(Pc). The heterotrimer showed additional bands with a rather complicated MCD pattern in the range from 25×10^3 to 29×10^3 cm^{-1}.[7] We had not given an assignment to these bands, but can now conclude that the extra bands are not of Pc-centered ($\pi-\pi^*$) transitions but of those which involve the electrons or orbitals having a large population on the alkoxy groups.

The First Oxidation Step Generating $[Pc_3Lu_2]^+$. The additions of equimolar amounts of phenoxathiin hexachloro-

(21) Used parameters are as follows: for carbon atoms, ionization potential of z ($2p_z$) orbital Ip = 11.22 eV, one-center Coulomb integral ($zz|zz$) = 10.60 eV, and Slater's orbital exponent ζ = 1.625; for nitrogen atoms, Ip = 14.51 eV, ($zz|zz$) = 13.31 eV, and ζ = 1.95.

(22) Pilcher, C.; Skinner, H. A. *J. Inorg. Nucl. Chem.* **1962**, *24*, 937.

(23) According to Pilcher and Skinner,[22] the ionization potential of a process $(t_1^2t_2t_3z) \rightarrow (t_1^2t_2t_3)$ is 14.51 eV, that of $(t_1t_2t_3z^2) \rightarrow (t_1t_2t_3z)$ 12.25 eV, and the electron affinity of $(t_1^2t_2t_3z) \rightarrow (t_1^2t_2t_3z^2)$ 1.20 eV. Here t_1, t_2, and t_3 are sp^2 hybrid orbitals and z is a $2p_z$ orbital. These are expressed by a one-electron term I_z and two-electron terms ($tt|zz$), ($tz|tz$), and ($zz|zz$) as follows: (i) $14.51 = -I_z - 4\{(tt|zz) - (tz|tz)/2\}$, (ii) $12.25 = -I_z - 3\{(tt|zz) - (tz|tz)/2\} - (zz|zz)$, and (iii) $1.20 = -I_z - 4\{(tt|zz) - (tz|tz)/2\} - (zz|zz)$. The effect of the donating charge q on the ionization potential (i) is expressed as $Ip = -I_z - (4 - q)\{(tt|zz) - (tz|tz)/2\} = 58.71 - 11.05(4 - q)$.

(24) Mataga, N.; Nishimoto, K. *Z. Phys. Chem.* (*Munich*) **1957**, *13*, 140.

(25) Moussavi, M.; De Cian, A.; Fischer, J.; Weiss, R. *Inorg. Chem.* **1988**, *27*, 1287.

(26) Maurice, D.; Head-Gordon, M. *J. Phys. Chem.* **1996**, *100*, 6131.

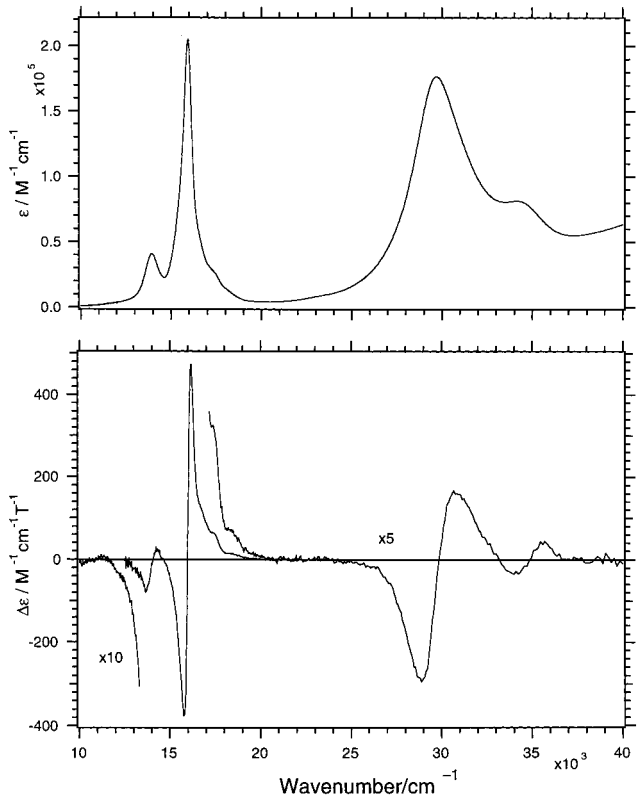

Figure 2. Electronic (top) and MCD spectra (bottom) of $Lu_2(Pc)_3$ in dichloromethane.

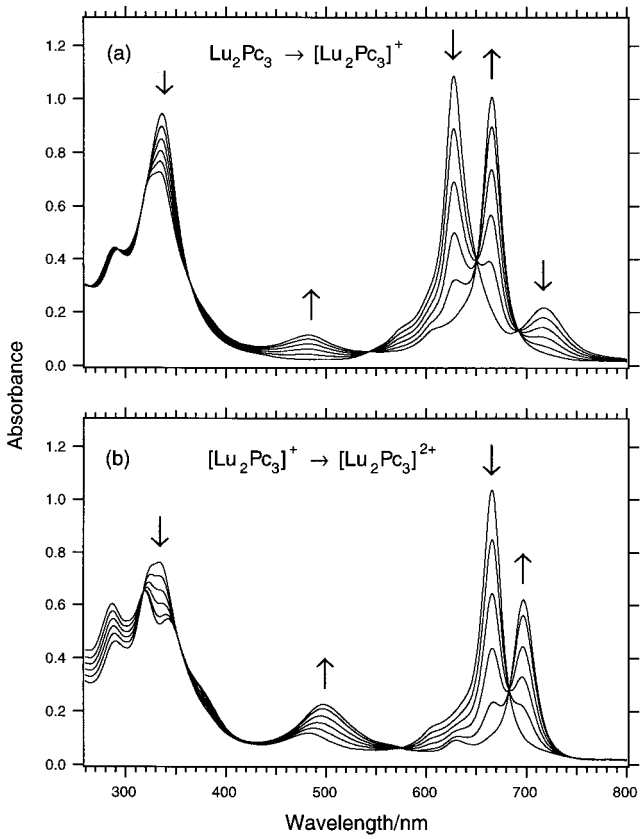

Figure 3. Absorption spectra for (a) the oxidation of $Lu_2(Pc)_3$ to $[Lu_2(Pc)_3]^+$ and (b) that of $[Lu_2(Pc)_3]^+$ to $[Lu_2(Pc)_3]^{2+}$, in dichloromethane by addition of phenoxathiin hexachloroantimonate solution in the same solvent. The initial concentration of $Lu_2(Pc)_3$ was 5.1×10^{-6} M. The concentrations of the oxidant were 5.1×10^{-6} M (top) and 1.0×10^{-5} M (bottom). Each spectrum corresponds to the addition of (a) 0.2 and (b) 0.4 equiv of the oxidant.

antimonate solution caused a change of the absorption spectrum keeping isosbestic points at 692, 650, 543, and 364 nm as shown in Figure 3a. This result indicates that the oxidation occurs stoichiometrically. The two Q bands of the neutral Pc_3Lu_2 disappeared, and a single Q band appeared at 15.0×10^3 cm^{-1} (665 nm). A band corresponding to the "fingerprint band" of Pc π-cation radicals appeared at 20.7×10^3 cm^{-1} (483 nm). The ESR spectrum in a frozen solution at 77 K (Figure 4) showed a signal at $g = 2.0020$ with 0.70 mT peak-to-peak width.

Figure 5 shows UV−vis and NIR absorption and MCD spectra of the oxidized species $[Lu_2(Pc)_3]^+$. The spectra have been corrected by subtracting the absorption of the reduced oxidant coexisting in the solution. The lowest energy band is the one labeled as **a** at 4.65×10^3 cm^{-1} (2150 nm). This band was unfortunately out of range of the MCD spectrometer used in this work. The Q band at 15.0×10^3 cm^{-1} shows an *A*-term dispersion ($A/D \approx +0.7\ \mu_B$,[27−29] μ_B = Bohr magneton). Between the two bands, several weak bands are observed. At the absorption maximums **g** at 9.9×10^3 cm^{-1} (1010 nm) and **e** at

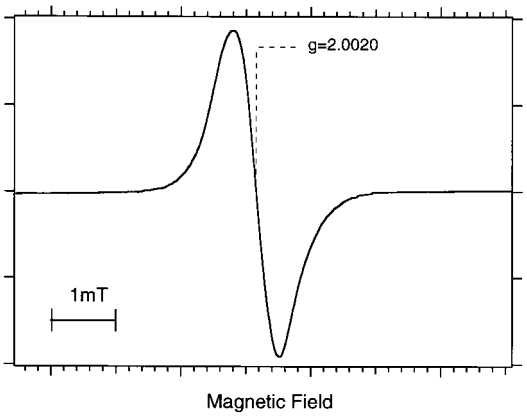

Figure 4. X-band ESR spectrum of $[Lu_2(Pc)_3]^+$ in a frozen solution in CH_2Cl_2 at 77 K.

12.7×10^3 cm^{-1} (790 nm), MCD shows positive slopes indicating normal (positive) *A* terms. Each of the bands should be assigned to a degenerate excited state. A rough estimate of the *A*/*D* value for **g** is $+0.5\ \mu_B$, and that for **e** is $+0.4\ \mu_B$.[29] The *A*-term contribution is absent or very small in the bands **b** (6.3×10^3 cm^{-1}), **c** (7.9×10^3 cm^{-1}), and **d** (8.9×10^3 cm^{-1}). In the region **f**, no distinct absorption maximum can be located.

(27) (a) Piepho, S. B.; Schatz, P. N. *Group Theory in Spectroscopy, With Application to Magnetic Circular Dichroism*; John Wiley & Sons, Inc.: New York, 1983; Chapter A-5. (b) Stephens, P. J.; Suëtaka, W.; Schatz, P. N. *J. Chem. Phys.* **1966**, *44*, 4592. (c) Schatz, P. N.; MaCaffery, A. J.; Suëtaka, W.; Henning, G. N.; Ritchie, A. B.; Stephens, P. J. *J. Chem. Phys.* **1966**, *45*, 722.

(28) *A*/*D* values were calculated assuming the Gaussian line shape[27] and using the equation $A/D = -\Delta\nu\Delta\epsilon/\{0.4807(8 \ln 2)^{1/2}\epsilon\}$. Here the *A*/*D* value is in Bohr magneton units, $\Delta\nu$ is the width between the minimum and maximum of the *A*-term dispersion (cm^{-1}), $\Delta\epsilon$ is the molar absorption coefficient for the left circularly polarized light minus that for right circularly polarized light at the minimum (normal *A*-term cases) or the maximum (negative *A*-term cases) (M^{-1} cm^{-1} T^{-1}), and ϵ is the molar absorption coefficient (M^{-1} cm^{-1}) of the absorption maximum. To remove the *B*-term and/or *C*-term contributions, the experimental $\Delta\epsilon$ values were determined by (minimum $\Delta\epsilon$ − maximum $\Delta\epsilon$)/2 for normal *A*-term cases and (maximum $\Delta\epsilon$ − minimum $\Delta\epsilon$)/2 for negative *A*-term cases.

(29) Assuming $\epsilon = 2 \times 10^5$, $\Delta\epsilon = -500$, and $\Delta\nu = 310$ for the Q band; $\epsilon = 2 \times 10^3$ (half the observed value at **h**), $\Delta\epsilon = -2$, and $\Delta\nu = 600$ for the band **g**; $\epsilon = 1 \times 10^3$ (half the observed value at **g**), $\Delta\epsilon = -1$, and $\Delta\nu = 430$ for the band **e**; $\epsilon = 2.3 \times 10^4$, $\Delta\epsilon = 2$, and $\Delta\nu = 1500$ for the band **h**.

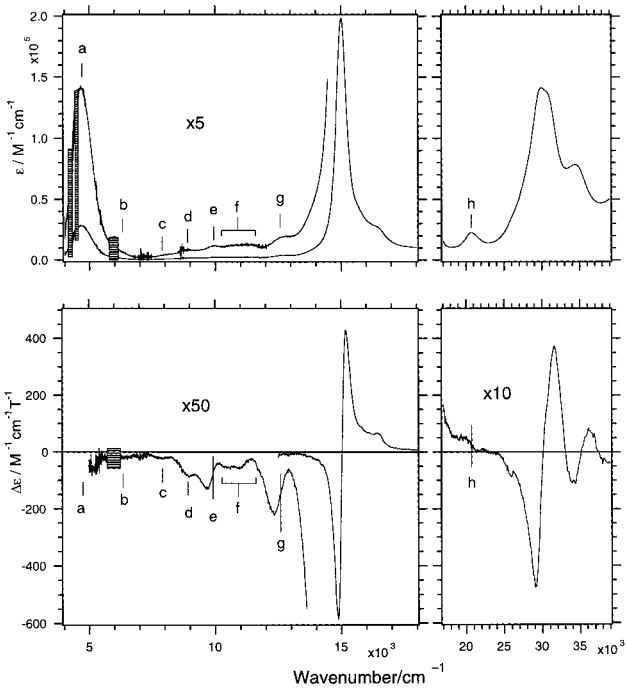

Figure 5. Electronic (top) and MCD spectra (bottom) of $[Lu_2(Pc)_3]^+$ in dichloromethane. The regions where the interference of the solvent could not be compensated are masked by striped rectangles.

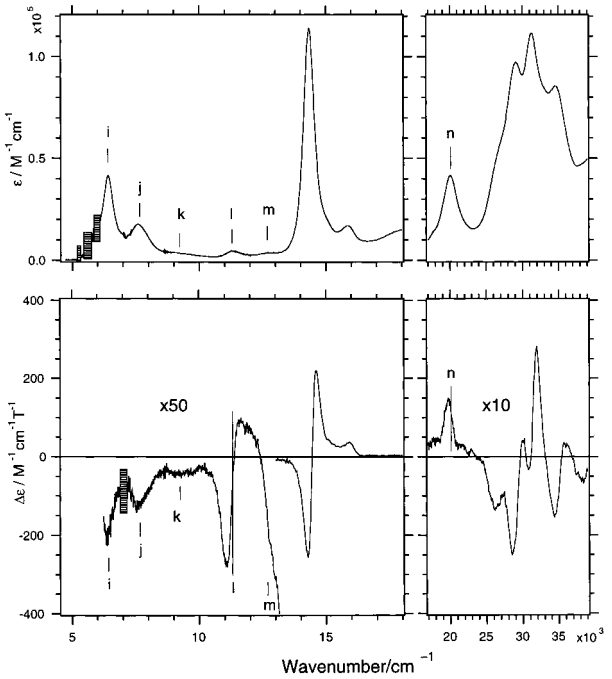

Figure 6. Electronic (top) and MCD spectra (bottom) of $[Lu_2(Pc)_3]^{2+}$ in dichloromethane. The regions where the interference of the solvent could not be compensated are masked by striped rectangles.

The band **h** at 20.7×10^3 cm^{-1} should be closely related to the bands which are seen in the Pc dimer radical $Lu(Pc)_2$[15,20] and monomeric Pc radicals[13,30] in the same energy region. The MCD shows a negative slope at the absorption maximum. This suggests the presence of a contribution of a negative *A* term. If it is the case, the *A*/*D* value is estimated at ca. -0.1 μ_B.[29]

In the B-band region, at least two bands at 29.6×10^3 cm^{-1} (338 nm) and 31.0×10^3 cm^{-1} (323 nm) (the wavelengths were determined by a second-derivative spectrum measurement) are present. The MCD indicates an *A*-term dispersion for each band.

Since the $[Lu_2(Pc)_3]^+$ is in a doublet state, each band contains an MCD *C*-term contribution, which is inversely proportional to the temperature. An examination of the temperature dependence of the MCD spectrum is necessary to determine the amount of such a contribution.

The Second Oxidation Step Generating $[Pc_3Lu_2]^{2+}$. An absorption spectral change through the second oxidation step is presented in Figure 3b. This step proceeded somewhat less efficiently than the first one. In each of the several attempts we made, 1.2—2.0 times the equimolar amount of the oxidant was required for the completion of this step. This is probably due to the water remaining in the solvent and/or entering the cell during the addition of the oxidant solution. However, in each attempt the spectral change took place keeping clear isosbestic points at 683, 574, and 352 nm.

The two-electron-oxidation product was ESR silent in frozen solution at 77 K. This indicates that the unpaired electron in the SOMO of $[Lu_2(Pc)_3]^+$ is removed by the oxidation to yield a diamagnetic species.

The lowest NIR bands of $[Lu_2(Pc)_3]^{2+}$ are observed at 6.4×10^3 cm^{-1} (1560 nm, labeled as **i** in Figure 6), 7.6×10^3 cm^{-1} (1315 nm, **j**) and ca. 9.3×10^3 cm^{-1} (ca. 1080 nm, **k**). These bands show only *B* terms in MCD. The band at 11.3×10^3 cm^{-1} (885 nm, **l**) shows a clear *A*-term dispersion ($A/D \approx 0.4$ μ_B[31]). In contrast to the presence of two *A*-term bands in $[Lu_2(Pc)_3]^+$, there is only one such band in $[Lu_2(Pc)_3]^{2+}$ in the NIR region. A less distinct band is observed at 12.8×10^3 cm^{-1} (783 nm, **m**).

The single Q band is red-shifted to 14.3×10^3 cm^{-1} (697 nm) and decreases its intensity. Again its MCD shows an *A* term ($A/D \approx 0.6$ μ_B[31]). The band at 15.8×10^3 cm^{-1} (631 nm) should be assigned to a vibronic structure of the main Q band.

The "fingerprint band" shifts to 20.1×10^3 cm^{-1} (497 nm) and increases its intensity. The MCD shows a rather unusual pattern. At a glance the MCD maximum might seem to be a *B* term. However, the wavenumber of the MCD maximum does not match that of the absorption band (shown by the lines labeled as "**n**"), and the width of the MCD peak is narrower than that of the absorption band. The MCD pattern actually can be viewed as a *negative A* term rather than a *B* term. If this is the case, its *A*/*D* value is roughly estimated at -0.2 μ_B.[31]

In the B-band manifold, several absorption maximums are observed at 26.5×10^3 cm^{-1} (377 nm), 29.1×10^3 cm^{-1} (343 nm), 31.3×10^3 cm^{-1} (320 nm), and 34.8×10^3 cm^{-1} (287 nm). Each of the bands shows an *A*-term dispersion in MCD.

The SCF-MO-CI Calculational Results and Band Assignments. Figure 7 presents calculated π-MO energy levels for $Lu_2(Pc)_3$, $[Lu_2(Pc)_3]^+$, and $[Lu_2(Pc)_3]^{2+}$.[32] Each of the three HOMOs of $Lu_2(Pc)_3$ can be approximated by a linear combination of three monomeric HOMOs: the $3a_{1u}$, $2a_{2g}$, and $4a_{1u}$ orbitals correspond to a bonding linear combination, a nonbonding combination, and an antibonding combination, respectively.[10] This is also the case for the LUMOs: the $11e_g$, $6e_u$, and $12e_g$ orbitals are roughly viewed as consisting of monomeric LUMO $6e_g$ orbitals and have bonding, nonbonding, and antibonding character, respectively.[10]

(30) (a) Nyokong, T.; Gasyna, Z.; Stillman, M. J. *Inorg. Chem.* **1987**, *26*, 548. (b) Nyokong, T.; Gasyna, Z.; Stillman, M. J. *Inorg. Chem.* **1987**, *26*, 1087. (c) Ough, E.; Gasyna, Z.; Stillman, M. J. *Inorg. Chem.* **1991**, *30*, 2301.

(31) Assuming $\epsilon = 1.1 \times 10^5$, $\Delta\epsilon = -240$, and $\Delta\nu = 310$ for the Q band; $\epsilon = 4.5 \times 10^3$, $\Delta\epsilon = -3.7$, and $\Delta\nu = 600$ for the band **l**; $\epsilon = 4 \times 10^4$, $\Delta\epsilon = 6$, and $\Delta\nu = 1500$ for the band **n**.

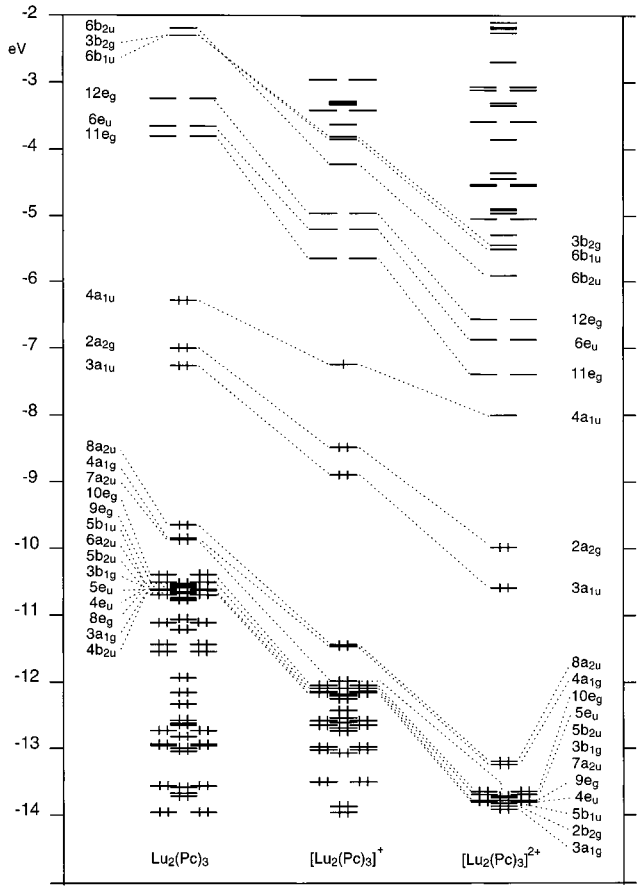

Figure 7. MO energy levels[32] of $Lu_2(Pc)_3$, $[Lu_2(Pc)_3]^+$, and $[Lu_2(Pc)_3]^{2+}$.

Assignments of the bands below the Q band are basically unchanged from those previously presented for (Pc)Lu(CRPc)Lu(Pc).[10] Out of nine singly excited configurations generated from the three HOMOs and three LUMOs, five configurations have nonzero transition dipole moments (arrows in Figure 8a). The configurations denoted by "2", "3", and "4" are relatively close in energy and strongly couple though configuration interaction. The band at 15.9×10^3 cm^{-1} is attributed to the $4E_u$ state, and its largest component is $|11e_g \leftarrow 3a_{1u}\rangle$ ("4", bonding ← bonding character). The band at 13.9×10^3 cm^{-1} is the $3E_u$, whose largest component is $|6e_u \leftarrow 2a_{2g}\rangle$ ("3", nonbonding ← nonbonding character). The band observed as a tail extending from ca. 13×10^3 cm^{-1} to the lower energy is the $2E_u$ state, whose largest component is $|12e_g \leftarrow 4a_{1u}\rangle$ ("2", antibonding ← antibonding). To the $1E_u$ state, which is predominantly HOMO-to-LUMO transition "1", the weak band observed in (Pc)Lu(CRPc)Lu(Pc) at 7×10^3 cm^{-1} was assigned in the previous study.[10]

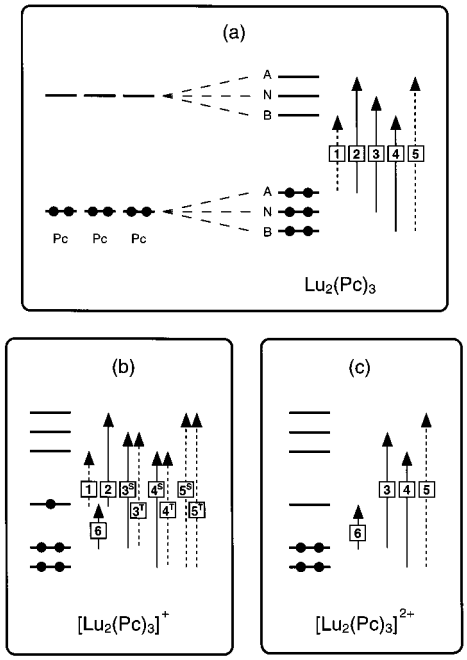

Figure 8. Schematic representations of excited configurations involved in the allowed lowest excited states of (a) $Lu_2(Pc)_3$, (b) $[Lu_2(Pc)_3]^+$, and (c) $[Lu_2(Pc)_3]^{2+}$. The letters "B", "N", and "A" refer to bonding, nonbonding, and antibonding (corresponding to $3a_{1u}$, $2a_{2g}$, and $4a_{1u}$ orbitals and $11e_g$, $6e_u$, and $12e_g$ unoccupied orbitals) combinations of monomer MOs, respectively.

Ground and Excited States of $[Lu_2(Pc)_3]^+$. The SOMO of the first oxidation product $[Lu_2(Pc)_3]^+$ is the $4a_{1u}$ orbital, and the HOMO is the $2a_{2g}$ orbital. The ground state is $^2A_{1u}$. Electric-dipole-transition allowed excited states are ^2E_g and $^2A_{2g}$. The transition moment of a ^2E_g state is polarized in the x,y plane, on which the Pc's are laid, and that of a $^2A_{2g}$ state is polarized along the z axis, which is perpendicular the Pc plane. The HOMO-to-SOMO transition labeled as "6" in Figure 8b results in a $^2A_{2g}$ state, which is electric-dipole allowed. There are two kinds of excited configurations generated by the promotion of an electron from a doubly occupied orbital to a virtual orbital. The configurations of the first kind are defined by eq 3. The arrows "3^S", "4^S", and "5^S" in Figure 8b represent transitions which give the configurations of this category. The MO-basis expression for the transition dipole moment of a transition of this type is same as that of an excited singlet of a closed-shell species. Therefore actual values for the moments of the cation radical should be close to the counterparts of the neutral species as long as the coefficients of the MOs do not differ significantly between the two species. The configuration of the second kind is defined by eq 4. The configurations generated by the transitions "3^T", "4^T", and "5^T" in Figure 8b fall into this category. The values of their transition moments are 0. In this sense these configurations do not contribute to the spectral intensity, but each of them can acquire an intensity through configuration interaction.

Figure 9 presents the calculational results for excited doublet states of $[Lu_2(Pc)_3]^+$ with varied interplanar distances R. To date no X-ray crystallographic study for the complex has been reported. In a related triple-decker complex $Ce_2(OEP)_3$ (OEP = octaethylporphyrin), the distance between two adjacent planes is about 0.2 Å larger than that of the dimer radical $Ce(OEP)_2$.[4a]

(32) In Figure 7 the "orbital energies" of the ROHF MOs **c** are defined as the expectation values $\mathbf{c}^\dagger\mathbf{F}\mathbf{c}$ for the Fock matrix for the *doubly* occupied shell,

$$\mathbf{F} = \mathbf{h} + 2\mathbf{J}(\mathbf{R}_d) - \mathbf{K}(\mathbf{R}_d) + \mathbf{J}(\mathbf{R}_s) - \frac{1}{2}\mathbf{K}(\mathbf{R}_s)$$

Here $\mathbf{R}_d$ and $\mathbf{R}_s$ are density matrices for electrons of given spin in the doubly occupied and singly occupied shells, respectively. **J** and **K** are Coulomb and exchange matrices. **h** is a one-electron Hamiltonian matrix. In the actual SCF procedure the Fock matrix for the *singly* occupied shell is

$$\mathbf{F}_s = \mathbf{h} + 2\mathbf{J}(\mathbf{R}_d) - \mathbf{K}(\mathbf{R}_d) + \mathbf{J}(\mathbf{R}_s) - \mathbf{K}(\mathbf{R}_s)$$

The expectation value of the SOMO $4a_{1u}$ for $\mathbf{F}_s$ was −8.46 eV. The expectation value of the $4a_{1u}$ orbital for a matrix,

$$\mathbf{F}'_s = \mathbf{h} + 2\mathbf{J}(\mathbf{R}_d) - \mathbf{K}(\mathbf{R}_d) + \mathbf{J}(\mathbf{R}_s)$$

corresponds to the energy of the unoccupied counterpart of the SOMO and was calculated at −5.99 eV. The mean of the two values corresponds to the energy of the $4a_{1u}$ orbital in Figure 7.

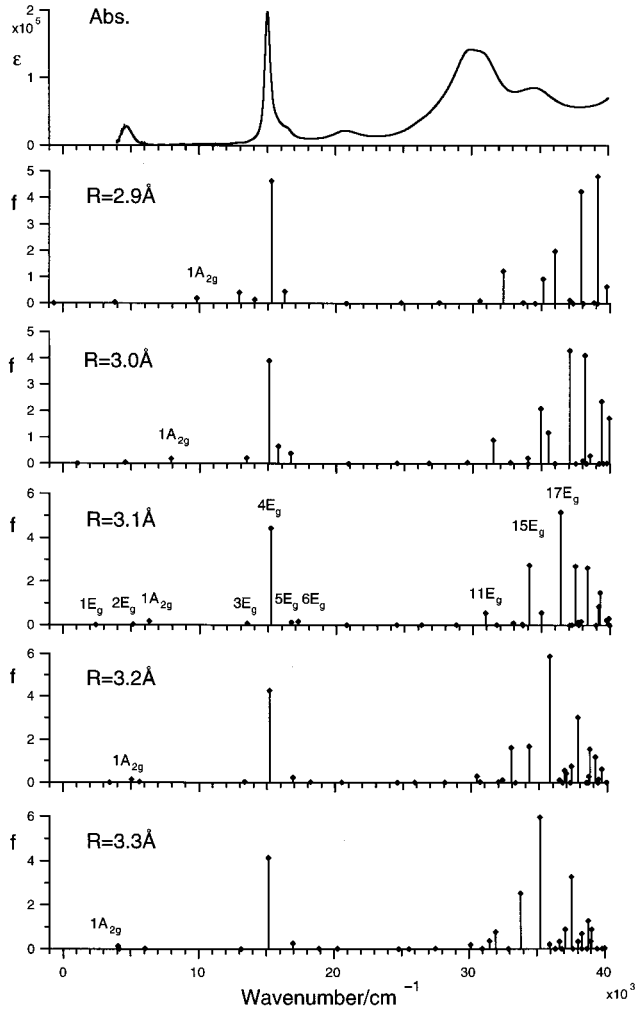

Figure 9. Calculated excitation energies and oscillator strengths of $[Lu_2(Pc)_3]^+$ with varied interplanar distances R and the observed absorption spectrum of $[Lu_2(Pc)_3]^+$ in dichloromethane (top).

Here each of the planes is defined by the eight carbon atoms next to the nitrogen atoms in the porphyrin. The cause of the difference may be that the central macrocycle in the trimer is flattened whereas both the macrocycles in the dimer are warped inward at the coordinating nitrogen atoms. It is likely that the interplanar distance in the Pc trimer is also larger to a similar degree than that of the Pc dimer considering the analogous structural relation. Table 1 shows details of the result obtained assuming the interplanar distance to be 3.1 Å, which is 0.2 Å larger than that of $Lu(Pc)_2$ (2.9 Å)[15] and 0.1 Å larger than that of $[Lu(Pc)_2]^-$ (3.0 Å).[25]

The $1A_{2g}$ state, which is predominantly described as the HOMO-to-SOMO transition, is calculated in the NIR region. The oscillator strength of the state is the largest among those below 10×10^3 cm^{-1}. The band **a** is assigned to this state. The calculation predicted that the band shifts to the red with an increase of interplanar distance.

An E_g state with a prominently large intensity is predicted at about 15×10^3 cm^{-1}. The state is the fourth E_g state in the cases $R \geq 3.0$ Å. The Q band at 15.0×10^3 cm^{-1} should be assigned to this state. Three degenerate E_g bands are predicted below the Q band with $R \geq 3.0$ Å. The oscillator strengths of the three E_g states are significantly smaller than that of the $4E_g$ state. The MCD *A*/*D* ratios for all four E_g states are positive. The band **g**, which shows a positive MCD *A* term, should be assigned to the $3E_g$ state considering the agreement with the observed energy. Energies of $1E_g$ and $2E_g$ states are highly dependent on the assumed interplanar distance: both states are below the $1A_{2g}$ state in $R = 3.1$ Å but above the state in $R = 3.3$ Å. In our calculation the relative energies of these states do not seem reliable. Judging by the observed positive MCD *A* term the band **e** should be assigned to the $2E_g$ state. The $1E_g$ state should correspond to another band with a positive MCD *A* term. Considering that in the neutral Pc trimer (Pc)Lu(CRPc)-Lu(Pc) the lowest energy band (essentially HOMO−LUMO excitation) is observed at 7×10^3 cm^{-1},[10] it is probable that the corresponding SOMO−LUMO transition band, namely, the $1E_g$ band, is below 7×10^3 cm^{-1} and hidden by the bands **a** and **b**.

For an assignment of each of the bands **b**, **c**, **d**, and **f**, two hypotheses are possible. One possibility is to assign a band to belong to a vibronic progression of an allowed state. Another possibility is to assume that a band derives from an E_u state. When the D_{4h} structure deforms by such a distortion that the center of inversion is removed, for example a twisting of the two outer Pc rings in opposite directions around the *z* axis, an E_u state in D_{4h} becomes an E state and a non-zero transition moment is obtained. Both possibilities are acceptable for **b** and **f**. Given that the first assumption is true, **b** is a vibronic band of **a**, and bands in the **f** region belong to a vibronic progression of **e**. For **c** and **d**, only the second possibility is reasonable because there is no intense E_g band near and below them.

The calculation well reproduced the "disappearance" of one of the two Q bands on the oxidation of $Lu_2(Pc)_3$. The $4E_g$ state involves a nearly 50/50 mixing of "4^S" ($|S\ 11e_{gxz} \leftarrow 3a_{1u}\rangle$) and "$3^S$" ($|S\ 6e_{ux} \leftarrow 2a_{2g}\rangle$) configurations as the leading component. The $3E_g$ state also has the same two leading configurations with a different sign combination of the coefficients. This contrasts with the neutral trimer case: the "4" configuration comprises ca. 60% of the $4E_u$ state of the $Lu_2(Pc)_3$, and the "3" comprises ca. 70% of the $3E_u$ state.[10] The removal of an electron from the HOMO brings the "3^S" and "4^S" configurations closer in energy and leads to a nearly equivalent mixing of the two. The transition moments of the two configurations take similar values. Thus the plus combination of the configurations gains net transition intensity whereas the minus combination results in a reduced intensity by the cancellation of the moments.

The band **h** should be attributed to a state characterized by transitions from low-lying e_g orbitals to the SOMO as in monomeric Pc cation radicals[13] and the dimer radical $Lu(Pc)_2$.[20] The $15E_g$ state has such a character. Its main components are $|D\ 4a_{1u} \leftarrow 9e_g\rangle$ and $|D\ 4a_{1u} \leftarrow 10e_g\rangle$ configurations. The calculation reproduced the observed relatively large intensity. The calculated *A*/*D* value of the state is considerably smaller than those of the bands below this state. The smallness agrees with the experiment, but the sign does not. The disagreement is probably due to the error in the balance between the coefficients of the two main configurations.

In the higher energy region the density of the E_g states increases, and a simple characterization becomes impossible because of the mixing of an increasing number of configurations. Moreover, the configurations which are not included in the present calculations should become more important in this region. Therefore in this paper we do not discuss the bands in this region.

Ground and Excited States of $[Lu_2(Pc)_3]^{2+}$. The second oxidation removes the electron in the SOMO. The $4a_{1u}$ orbital becomes the LUMO in $[Lu_2(Pc)_3]^{2+}$. E_u and A_{2u} excited states are electric-dipole-transition allowed. An E_u state has an *x*,*y*-polarized transition moment, and an A_{2u} state has a *z*-polarized

Table 1. Calculated Excitation Energies, Oscillator Strengths *f*, MCD *A*/*D* Ratios, and Wavefunctions of Doublet Excited States of $[Pc_3Lu_2]^+$ with an Interplanar Distance of 3.1 Å

	$\bar{\nu}$/cm^{-1}	*f*	*A*/*D*[a]	wavefunctions
$1E_{gxz}$	2.4	0.0001	0.93	$0.79\|D\ 11e_{gxz} \leftarrow 4a_{1u}\rangle - 0.44\|T\ 6e_{ux} \leftarrow 2a_{2g}\rangle - 0.29\|T\ 12e_{gxz} \leftarrow 3a_{1u}\rangle + ...$
$1E_{ux}$	3.4			$0.59\|D\ 6e_{ux} \leftarrow 4a_{1u}\rangle - 0.49\|T\ 6e_{ux} \leftarrow 3a_{1u}\rangle - 0.45\|T\ 12e_{gxz} \leftarrow 2a_{2g}\rangle + ...$
$2E_{gxz}$	5.2	0.015	0.87	$0.56\|D\ 12e_{gxz} \leftarrow 4a_{1u}\rangle - 0.50\|D\ 11e_{gxz} \leftarrow 4a_{1u}\rangle - 0.45\|T\ 6e_{ux} \leftarrow 2a_{2g}\rangle + ...$
$1A_{2g}$	6.3	0.17		$0.99\|D\ 4a_{1u} \leftarrow 2a_{2g}\rangle + ...$
$1A_{1u}$	8.2			$0.99\|D\ 4a_{1u} \leftarrow 3a_{1u}\rangle + ...$
$2E_{ux}$	9.4			$0.97\|S\ 11e_{gxz} \leftarrow 2a_{2g}\rangle + ...$
$3E_{ux}$	13.1			$0.56\|S\ 12e_{gxz} \leftarrow 2a_{2g}\rangle + 0.55\|T\ 11e_{gxz} \leftarrow 2a_{2g}\rangle + 0.46\|D\ 6e_{ux} \leftarrow 4a_{1u}\rangle + ...$
$3E_{gxz}$	13.5	0.042	0.94	$0.68\|S\ 11e_{gxz} \leftarrow 3a_{1u}\rangle - 0.56\|S\ 6e_{ux} \leftarrow 2a_{2g}\rangle - 0.34\|S\ 12e_{gxz} \leftarrow 3a_{1u}\rangle + ...$
$4E_{gxz}$	15.2	2.2	1.5	$0.60\|S\ 11e_{gxz} \leftarrow 3a_{1u}\rangle + 0.56\|S\ 6e_{ux} \leftarrow 2a_{2g}\rangle + 0.34\|D\ 12e_{gxz} \leftarrow 4a_{1u}\rangle + ...$
$4E_{ux}$	16.5			$0.61\|S\ 6e_{ux} \leftarrow 3a_{1u}\rangle - 0.57\|T\ 11e_{gxz} \leftarrow 2a_{2g}\rangle + 0.32\|S\ 12e_{gxz} \leftarrow 2a_{2g}\rangle + ...$
$5E_{gxz}$	16.7	0.062	0.88	$0.66\|T\ 11e_{gxz} \leftarrow 3a_{1u}\rangle + 0.49\|S\ 12e_{gxz} \leftarrow 3a_{1u}\rangle - 0.38\|S\ 6e_{ux} \leftarrow 2a_{2g}\rangle + ...$
$6E_{gxz}$	17.2	0.085	0.90	$0.69\|T\ 6e_{ux} \leftarrow 2a_{2g}\rangle + 0.47\|D\ 12e_{gxz} \leftarrow 4a_{1u}\rangle - 0.34\|S\ 6e_{ux} \leftarrow 2a_{2g}\rangle + ...$
$7E_{gxz}$	20.8	0.003	0.86	$0.75\|S\ 12e_{gxz} \leftarrow 3a_{1u}\rangle - 0.52\|T\ 11e_{gxz} \leftarrow 3a_{1u}\rangle - 0.29\|D\ 12e_{gxz} \leftarrow 4a_{1u}\rangle + ...$
$11E_{gxz}$	30.9	0.28	0.50	$0.71\|S\ 11e_{gyz} \leftarrow 8a_{2u}\rangle - 0.35\|D\ 4a_{1u} \leftarrow 8e_{gxz}\rangle + 0.33\|S\ 6e_{uy} \leftarrow 4a_{1g}\rangle + ...$
$15E_{gxz}$	34.1	1.4	0.03	$0.53\|D\ 4a_{1u} \leftarrow 9e_{gxz}\rangle - 0.43\|D\ 4a_{1u} \leftarrow 10e_{gxz}\rangle + 0.24\|T\ 6e_{ux} \leftarrow 2b_{2g}\rangle + ...$

[a] The unit of the values in the column is Bohr magneton.

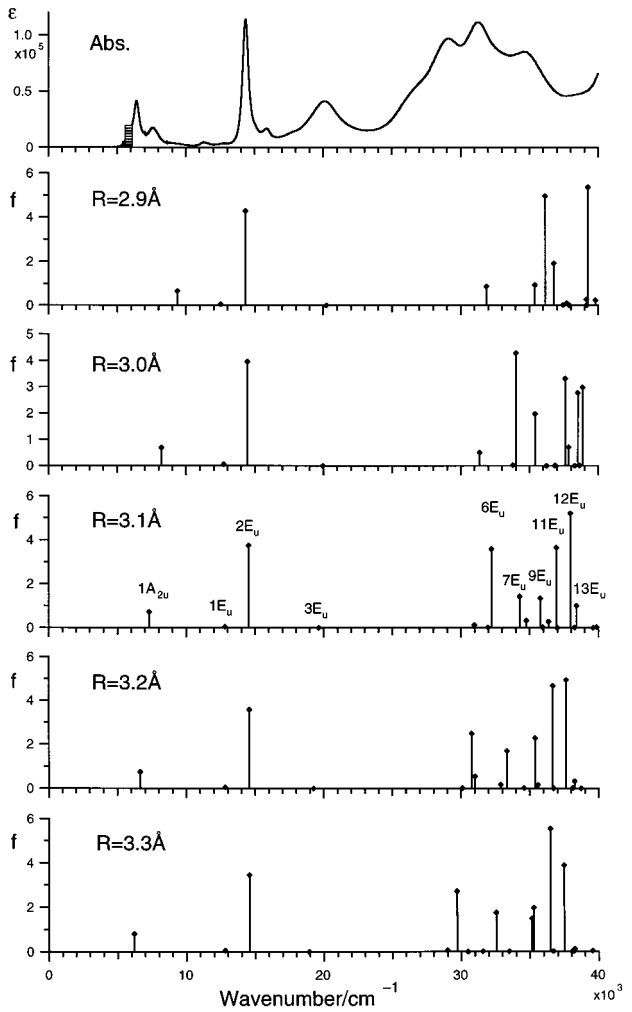

Figure 10. Calculated excitation energies and oscillator strengths of $[Lu_2(Pc)_3]^{2+}$ with varied interplanar distances *R* and the observed absorption spectrum of $[Lu_2(Pc)_3]^{2+}$ in dichloromethane (top).

moment. By the removal of the electron in the SOMO, the excitations "1" and "2" vanish from the possibilities (Figure 8c). The remaining excitations having a contribution in the region below the Q band are "3", "4", and "6".

The results of the CI calculations with varied interplanar distances are shown in Figure 10. The general picture below 20×10^3 cm^{-1} is unchanged in the region 2.9Å $\leq R \leq$ 3.3 Å except the large energy shift of the $1A_{2u}$ state. Table 2 shows the details of the case $R = 3.1$ Å. The Q band at 14.3×10^3 cm^{-1} and the NIR band **l** with a positive MCD *A* term are assigned to $2E_u$ and $1E_u$ states, respectively. The two states hold the same relationship as that between the $4E_g$ and $3E_g$ states of $[Lu_2(Pc)_3]^+$: each state has a near 50:50 linear combination of the "3" and "4" configurations ("3^S" and "4^S" in $[Lu_2(Pc)_3]^+$) leading to a greater intensity in the higher energy state and an extremely small intensity in the lower energy state. The band **m** is assigned to a vibronic band of the $1E_u$ state because no electronic state is predicted between $1E_u$ and $2E_u$ states.

The lowest excited state is $1A_{2u}$, which is characterized as the HOMO-to-LUMO transition "6". The lowest energy band **i** is assigned to the state. The bands **j** and **k** are likely to belong to the vibronic progression of the $1A_{2u}$ state. However, a possibility that the weaker band **k** is derived from the $1E_g$ state, which is predicted just above the $1A_{2u}$ state, cannot be excluded because the state can obtain an intensity if ring rotations which remove the center of inversion occur.

The $6E_u$ state in $R \leq 3.1$ Å or the $5E_u$ state in $R \geq 3.2$ Å has a large intensity and contains two configurations generated by an excitation from a low-lying e_g occupied orbital to the LUMO $4a_{1u}$ orbital, i.e., $|4a_{1u} \leftarrow 9e_g\rangle$ and $|4a_{1u} \leftarrow 10e_g\rangle$, as main components. The band **n** should be assigned to the state. The calculations predict a negative *A*/*D* value, which agrees with the observed negative MCD *A*-term pattern. Each of the states $7E_u$ and $8E_u$ ($R = 3.1$ Å) also has an excited configuration from an occupied e_g orbital to the LUMO and an intensity which is not negligible. There remains a possibility that either or both of the two states are included in the fingerprint band manifold.

Conclusion

We reported an alternative synthetic route to $Lu_2(Pc)_3$. Heating of a monomeric lutetium Pc complex $PcLu(CH_3COO)(H_2O)_2$ in vacuo produced the Pc trimer in good yield. The purification of $Lu_2(Pc)_3$ was achieved by chromatographic means. $Lu_2(Pc)_3$ was oxidized to $[Lu_2(Pc)_3]^+$ and then to $[Lu_2(Pc)_3]^{2+}$ by the reaction with phenoxathiin hexachloroantimonate in dichloromethane solution. Each of the steps occurred keeping isosbestic points.

The electronic and MCD spectra of $Lu_2(Pc)_3$, $[Lu_2(Pc)_3]^+$, and $[Lu_2(Pc)_3]^{2+}$ in the region over UV, vis, and NIR were presented for the first time. Assignments of the absorption bands were discussed using CI calculations in ROHF MO basis for $[Lu_2(Pc)_3]^+$ and in RHF MO basis for $[Lu_2(Pc)_3]^{2+}$.

The one-electron-oxidation product $[Lu_2(Pc)_3]^+$ showed a relatively intense band at 4.65×10^3 cm^{-1} (**a** in Figure 5). This

Table 2. Calculated Excitation Energies, Oscillator Strengths *f*, MCD *A*/*D* Ratios, and Wavefunctions of Singlet Excited States of $[Pc_3Lu_2]^{2+}$ with an Interplanar Distance of 3.1 Å

	$\bar{\nu}$/cm^{-1}	*f*	*A*/*D*[a]	wavefunctions
$1A_{2u}$	7.3	0.71		$0.99\|4a_{1u} \leftarrow 2a_{2g}\rangle + ...$
$1E_{gxz}$	7.7			$0.99\|11e_{gyz} \leftarrow 2a_{2g}\rangle + ...$
$1A_{1g}$	10.8			$0.99\|4a_{1u} \leftarrow 3a_{1u}\rangle + ...$
$1E_{ux}$	12.8	0.023	0.97	$0.72\|6e_{uy} \leftarrow 2a_{2g}\rangle - 0.65\|11e_{gyz} \leftarrow 3a_{1u}\rangle + 0.24\|12e_{gyz} \leftarrow 3a_{1u}\rangle + ...$
$2E_{ux}$	14.5	1.9	1.4	$0.73\|11e_{gyz} \leftarrow 3a_{1u}\rangle + 0.61\|6e_{uy} \leftarrow 2a_{2g}\rangle - 0.16\|6e_{ux} \leftarrow 4a_{1g}\rangle + ...$
$2E_{gxz}$	14.9			$0.89\|12e_{gyz} \leftarrow 2a_{2g}\rangle + 0.42\|6e_{uy} \leftarrow 3a_{1u}\rangle + ...$
$3E_{gxz}$	18.0			$0.90\|6e_{uy} \leftarrow 3a_{1u}\rangle - 0.43\|12e_{gyz} \leftarrow 2a_{2g}\rangle + ...$
$3E_{ux}$	19.6	0.002	0.86	$0.96\|12e_{gyz} \leftarrow 3a_{1u}\rangle - 0.25\|6e_{uy} \leftarrow 2a_{2g}\rangle + ...$
$4E_{ux}$	31.0	0.062	0.52	$0.68\|11e_{gxz} \leftarrow 8a_{2u}\rangle - 0.36\|4a_{1u} \leftarrow 10e_{gyz}\rangle + 0.32\|6e_{ux} \leftarrow 4a_{1g}\rangle + ...$
$4E_{gxz}$	31.4			$0.56\|11e_{gxz} \leftarrow 4a_{1g}\rangle - 0.52\|4a_{1u} \leftarrow 4e_{uy}\rangle + 0.38\|6e_{ux} \leftarrow 8a_{2u}\rangle + ...$
$5E_{ux}$	32.0	0.012	0.15	$0.68\|4a_{1u} \leftarrow 9e_{gyz}\rangle + 0.41\|4a_{1u} \leftarrow 10e_{gyz}\rangle + 0.32\|11e_{gxz} \leftarrow 8a_{2u}\rangle + ...$
$6E_{ux}$	32.2	1.8	−0.19	$0.75\|4a_{1u} \leftarrow 10e_{gyz}\rangle - 0.53\|4a_{1u} \leftarrow 9e_{gyz}\rangle + 0.17\|12e_{gyz} \leftarrow 5b_{1u}\rangle + ...$
$7E_{ux}$	34.3	0.72	0.24	$0.76\|4a_{1u} \leftarrow 7e_{gyz}\rangle + 0.40\|11e_{gxz} \leftarrow 7a_{2u}\rangle + 0.30\|11e_{gxz} \leftarrow 8a_{2u}\rangle + ...$
$8E_{ux}$	34.8	0.16	−0.097	$0.80\|4a_{1u} \leftarrow 8e_{gyz}\rangle - 0.35\|11e_{gxz} \leftarrow 8a_{2u}\rangle + 0.29\|11e_{gyz} \leftarrow 4b_{1u}\rangle + ...$
$9E_{ux}$	35.8	0.68	0.15	$0.46\|11e_{gxz} \leftarrow 5b_{2u}\rangle - 0.42\|11e_{gxz} \leftarrow 7a_{2u}\rangle - 0.34\|4a_{1u} \leftarrow 9e_{gyz}\rangle + ...$

[a] The unit of the values in the column is Bohr magneton.

band was assigned to the $1A_{2g}$ state, which has a transition moment perpendicular to the Pc planes. In the Q-band region only one intense band was observed, in contrast to the two bands in the neutral $Lu_2(Pc)_3$. The single Q band was assigned to the $4E_g$ state, which mainly is composed of a near 50/50 mixing of "4^S" ($|S\ 11e_{gxz} \leftarrow 3a_{1u}\rangle$) and "$3^S$" ($|S\ 6e_{ux} \leftarrow 2a_{2g}\rangle$) configurations. The two configurations are also included in the $3E_g$ state but with a different sign combination, which leads to an extremely diminished intensity. The weak band **g** associated with a positive MCD *A* term at 9.9×10^3 cm^{-1} is attributed to the $3E_g$ state. Another weak band **e** with a positive *A* term at 12.7×10^3 cm^{-1} is assigned to the $2E_g$ state. To the "fingerprint" band **h**, the state which has a large intensity and has $|D\ 4a_{1u} \leftarrow 9e_g\rangle$ and $|D\ 4a_{1u} \leftarrow 10e_g\rangle$ as the main components should be attributed.

In the second oxidation product $[Lu_2(Pc)_3]^{2+}$, the lowest energy band $1A_{2u}$ was observed at 6.4×10^3 cm^{-1} (**i** in Figure 6) with two distinct vibronic bands at 7.6×10^3 cm^{-1} (**j**) and 9.3×10^3 cm^{-1} (**k**). None of the three bands showed an MCD *A* term. This indicates the state's nondegenerate nature. In the Q-band region, a single intense band was observed as in the monocation. Below the Q band, there was only one band showing an MCD *A* term (**l**). The decrease of bands in the NIR region is attributed to the decrease in possible excited configurations. The two configurations "3" and "4" again form 50/50 combinations to result in an intense band ($2E_g$ state) and a weak band ($1E_g$ state). The Q band is assigned to the $2E_g$ state and the band **l** to the $1E_g$ state. The "fingerprint" band **n** is attributed to the state whose main components are $|4a_{1u} \leftarrow 9e_g\rangle$ and $|4a_{1u} \leftarrow 10e_g\rangle$. The calculation predicted that the state has a negative *A*/*D* value and a large absorption intensity, both of which agree with the experimental result.

Acknowledgment. This work was partially supported by a Grant-in-Aid for Science Research No. 10740303 from the Ministry of Education, Science, Sports and Culture in Japan. The authors are grateful to Professor Hideyo Matsuzawa at Kitasato University for measurements of MCD spectra in the NIR region.

IC981463X